Lasers in Surgery and Medicine 18:100–108 (1996)

Temperature and Pressure Effects During Erbium Laser Stapedotomy

Hans Pratisto, MS, Martin Frenz, PhD, Michael Ith, MS, Valerio Romano, PhD, Dominik Felix, PhD, Rudolf Grossenbacher, MD, Hans J. Altermatt, MD, and Heinz P. Weber, PhD

Institutes of Applied Physics (H.P., M.F., M.I., V.R., H.P.W.) and Pathology (H.J.A.) and Division of Neurobiology, Zoological Institute (D.F.), University of Berne, Berne, Switzerland; ENT-Department, Kantonsspital St. Gallen, St. Gallen, Switzerland (R.G.)

Background and Objectives: **Laser-assisted stapedotomy has become a well-established alternative to the mechanical drilling method. The goal of this study is to quantify the mechanical and thermal tissue effects and to determine optimum erbium laser parameters for safe clinical treatment.**
Study Design/Materials and Methods: **On an inner ear model, time-resolved pressure measurements and Schlieren optical flash photography were performed during the perforation of the stapes foot plate using an erbium laser at 2.79 μm. The laser radiation was transmitted via an optical zirconium fluoride fiber. The laser-treated foot plates were investigated by light microscopy and scanning electron microscopy to visualise the laser-induced tissue effects.**
Results: **Perforation of the stapes foot plate can be performed with a few erbium laser pulses with high precision and a thermal damage zone of <10 μm. Strong pressure transients were found to be generated by the bone ablation process and the collapse of a vapor channel created in the perilymph after fenestration.**
Conclusion: **From the comparison of the laser-induced pressure with the limit graph to avoid hearing defects published by Pfander, an unobjectionable use of the erbium laser is deduced for fluences <10 J/cm^2. The erbium laser seems to represent an ideal instrument for middle ear surgery with all the advantages (precision, fiber optic transportable, high ablation efficiency, safety) desired for clinical application.**

Key words: bone ablation, cavitation bubble, inner ear model, IR-laser, PVDF pressure transducer

INTRODUCTION

The use of lasers in otolaryngology has become well established over the last two decades. Especially in the treatment of otosclerosis, where precise no-touch fenestration of the stapes foot plate is required, lasers provide an attractive alternative to mechanical drilling methods [1–6]. The major advantage using lasers to produce a precise hole in the stapes foot plate is the absence of direct contact, which eliminates the risk of foot plate mobilisation that causes rapid compression or decompression of the inner ear structures, which may lead to sensorineural hearing impairment. Additionally, bleeding may be reduced by the coagulation properties of the radiant energy, and the accuracy of the treatment is enhanced by the strong focusing properties of a laser beam. Today, Argon, KTP, and CO_2 lasers are already in clinical use for this procedure, although all of them are still controversial in the literature [7–9]. The interaction between tissue and visible laser light is strongly determined by the pigmen-

Accepted for publication November 28, 1994.

Address reprint requests to Dr. M. Frenz, Institute of Applied Physics, University of Berne, Sidlerstrasse 5, CH-3012 Berne, Switzerland.

tation properties of the tissue. At low bone pigmentation, the absorption and therefore the ablation efficiency is extremely low. As a result, the laser radiation can penetrate through the bone, which increases the risk of an iatrogenic injury of the Saccule and Utricle because of direct irradiation [10]. However, CO_2 laser radiation is strongly absorbed by bone and consequently has a high ablation efficiency, but its radiation cannot yet be guided through optical fibers. Today's surgical CO_2 lasers have an articulated arm connected to a micro manipulator for guiding the radiation from the laser to the narrow operation site, although this strongly confines the freedom of movement.

In contrast, the radiation of the Erbium laser, emitting in the near infrared, seems to be suitable for middle ear surgery [11]. It shows a high ablation efficiency [12, 13] of bone, and recently optical fibers have become available, through which the radiation can be transmitted [14].

The greatest potential risks for the inner ear during laser stapedotomy are the conversion of laser energy into heat in the vestibule, due to direct absorption of laser radiation or heat diffusion, and pressure fluctuations inside the cochlea caused by the explosive ablation process inherent in pulsed laser systems.

In this study we have quantified these risks by performing a series of experiments on an inner ear model using repetitive Erbium laser pulses delivered via an optical zirconium-fluoride (ZrF_4) fiber. In particular, using piezoelectric transducers, we measured at the inner ear model the laser-induced pressure, which is directly coupled into the "vestibule" during and after the perforation of the foot plate. The pressure fluctuations induced in the liquid were visualised using a Schlieren optical method. With this technique we also examined the effect of the strongly absorbing artificial perilymph as a "backstop" for the laser radiation and observed the dynamic and the geometric dimensions of a vapor channel created in the inner ear after fenestration of the stapes foot plate. The ablation depth and the tissue impairment following the laser procedure were assessed by histology and scanning electron microscopy (SEM).

MATERIALS AND METHODS

The experiments were performed with an Er:Cr:YSGG laser emitting at a wavelength of λ = 2.79 μm. The pulse duration of the laser operating in the free-running mode was τ = 200 μs. The laser pulse consists of a number of single spikes each with a pulse duration of ~2 μs. The pulse energy was varied by introducing attenuating glass plates into the beam. The radiation was delivered to the operation site via a zirconium-fluoride (ZrF_4) fiber with a core diameter of 350 μm. The end of the brittle ZrF_4 fiber was protected with a short, robust, low-OH quartz fiber end piece with a core diameter of 400 μm [15]. The distance between the distal fiber tip and the surface of the stapes foot plate placed on the inner ear model was either 500 μm (noncontact) or <100 μm (contact), where the contact between the fiber and the bone surface was realised by a water droplet.

The experiments were performed on an inner ear model. The liquid volume and the geometric dimensions of the inner ear model were chosen to be comparable to the human ear, whereby distilled water was used as artificial perilymph. The experimental setup is shown in Figure 1. The very fast temperature rise and associated pressure fluctuations were visualised with inverse Schlieren optical flash photography. For illumination we used a nano light flash lamp (white light) with a pulse duration of 20 ns (FWHM).

As biological material, cortical bone from the femur and stapes were removed from different patients at autopsy. The bone samples were kept refrigerated at −80°C until they were used in the experiment. Before laser treatment, the bone pieces were carefully brought to room temperature. It was thought that cortical bone from the femur has biological properties widely comparable with the bone of stapes. Therefore the determination of the ablation depth was performed on pieces of cortical bone of femurs, which were available easily and in large quantities. After laser treatment the bone fragments were fixed in formaline (10%) for light microscopy and in glutaraldehyde (3%) for SEM. Formalin-fixed material was decalcified for 4 days in EDTA (1'115 g ethylene diamine tetraacetate, 240 g citric acid, 5 L distilled water) and embedded in plastic; 2-μm-thick sections were stained with hematoxylin and eosin.

Pressure Measurements

Pressure transients induced by the pulsed laser system were detected with piezoelectric polyvinylidienefluoride pressure transducers (9-μm-thick PVDF-foil with a sensitive area of 0.25 ×

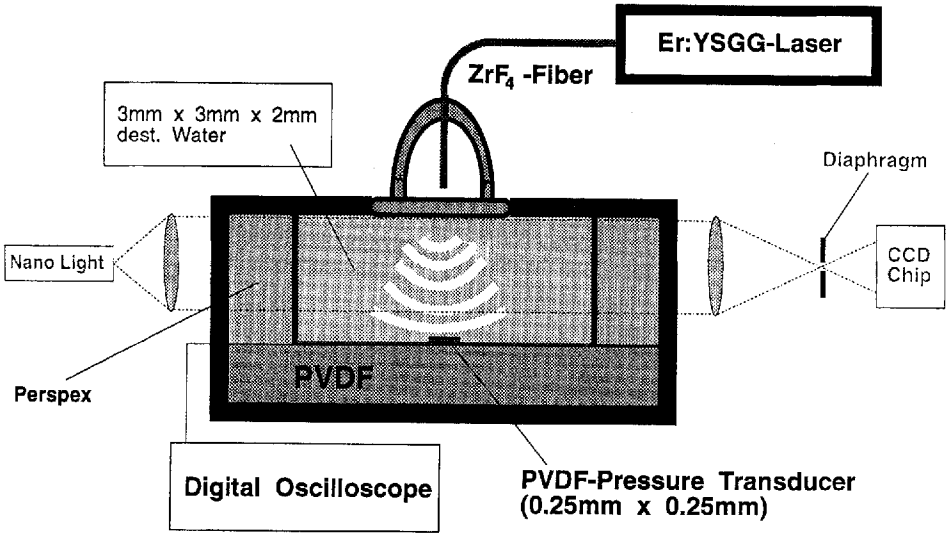

Fig. 1. Experimental setup of the inner ear model.

0.25 mm^2). Using a high impedance circuit, the output signal of the PVDF transducer is proportional to the applied pressure [16]. The PVDF-foil was adhered to an acoustic impedance matching stub (PVDF block) to avoid undesired acoustic reflections on the back of the transducer foil. Using this setup, pressure transients down to ~500 mbar could be directly resolved on an oscilloscope. To obtain a better representation of pressure amplitudes below 500 mbar, a low noise amplifier (gain 100, with a frequency range up to 1 MHz (3 dB point)) was used. To measure absolute pressure values, in spite of the small bandwidth of the amplifier, the measured values were corrected numerically by the frequency response characteristic of the amplifier. The distance between the ablated area and the pressure sensor was 2 mm (Fig. 1). The pressure transients were detected during and after the perforation of the stapes foot plate for both contact and noncontact applications.

RESULTS

Noncontact

The ablation depth in cortical bone as a function of the fluence measured at the fiber tip is shown in Figure 2. The ablation depth per pulse was calculated from the pulse energy and the number of pulses needed to drill a hole through a bone disk of well-known thickness. This procedure is feasible, because earlier measurements have shown that for the Erbium laser radiation the ablation depth is proportional to the number of pulses applied [17]. In good agreement with other investigators, we found that the ablation threshold is less than 5 J/cm^2 [11].

The temporal intensity profile of the laser pulse and the corresponding induced pressure signals measured in the liquid of the inner ear model during the bone ablation and after the foot plate fenestration performed in the noncontact mode is shown in Figure 3. For a laser pulse fluence at the fiber tip of 40 J/cm^2, the pressure amplitudes caused during the bone ablation are limited in time to the duration of the laser pulse and in strength to <500 mbar (Fig. 3, trace b). A comparison of the temporal intensity profile of the laser pulse (trace a) and the corresponding temporal pressure signal induced in the "vestibule" during the bone ablation reveals a clear correlation between each individual spike of the laser pulse and the pressure signal. If a laser pulse of 40 J/cm^2 is applied into an already existing perforation, additional strong pressure transients with amplitudes up to 9 bar occur after the end of the laser pulse (trace c, signals at 230 μs and 280 μs). With a laser pulse fluence of 10 J/cm^2, these strong pressure transients can now appear already during the laser pulse; however, their amplitude is reduced to <500 mbar (trace d). The pressure transients during the first 100 μs of the laser pulse caused by the explosive evaporation of water decrease thereby to a few tens of mbars.

The flash photographic pictures taken in the liquid below the stapes foot plate at 145 μs, 200

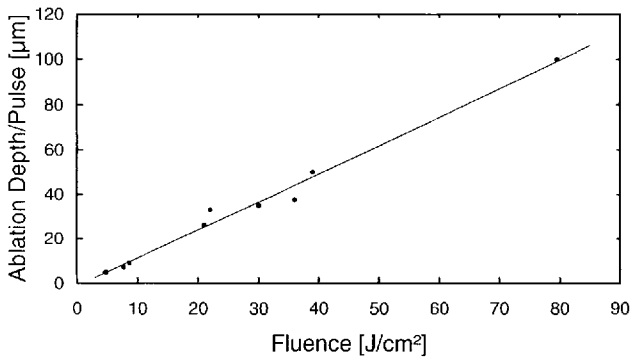

Fig. 2. Ablation depth per pulse as a function of the fluence for the Er:Cr:YSGG laser (λ = 2.79 µm, τ = 200 µs). The ablation threshold is <5 J/cm^2.

µs, and 240 µs after the beginning of a laser pulse (pulse duration τ = 200 µs), which was directly applied into the artificial perilymph with a fluence of 40 J/cm^2 are shown in Figure 4. Figure 4a shows the maximum size of the vapor channel. This picture reveals that using an erbium laser pulse of 40 J/cm^2, no damage can be induced by direct laser irradiation at a distance deeper than 1 mm below the stapes foot plate. Similar to the vapor bubble created by IR-laser radiation at the end of a submerged fiber [18, 19], the channel closes at the interface bone-liquid separating a vapor bubble (Fig. 4b). The remaining turbulent water is clearly seen as dark streaks around the bubble. This bubble collapses, which induces a strong pressure transient visualised in Figure 4c and indicated in the strong pressure transient of 9 bar (Fig. 3, trace c). The pressure transient at 280 µs after the beginning of the laser pulse is due to a second collapse following a rebound of the vapor bubble. For a laser fluence of 10 J/cm^2, the vapor channel was found to collapse a first time already during the laser pulse and a second time after reopening due to the remaining laser pulse energy. These two collapses cause the two pressure transients of about 450 mbar shown in Figure 3 (trace d). It should be mentioned that although the dynamics of the bubble expansion is quite reproducible, the moment of its collapse or even more the collapse of the rebound strongly depends on the bubble size and the geometry. Therefore a jitter of several tens of microseconds was found even if constant laser parameters were used.

Contact

The pressure signal following a laser pulse with a fluence of 10 J/cm^2 applied in contact after

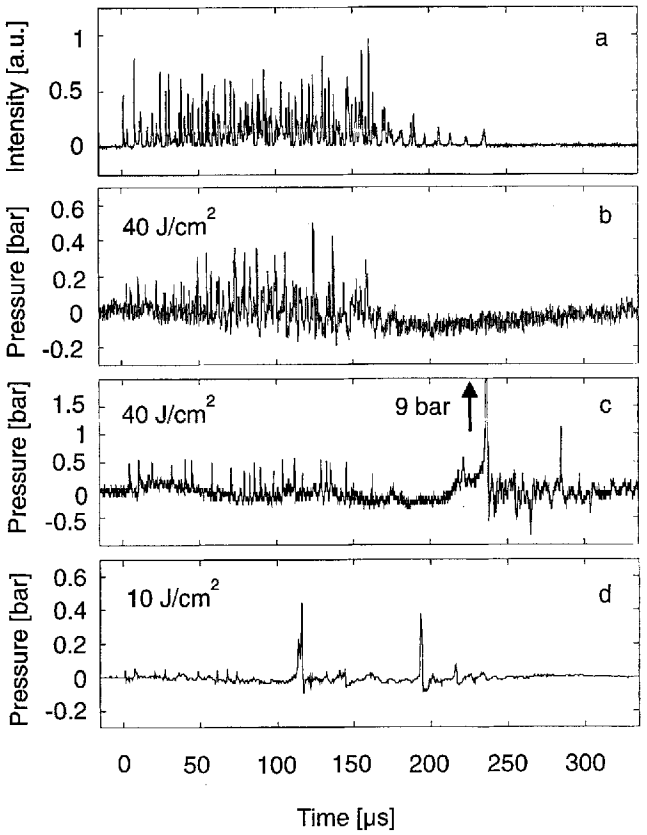

Fig. 3. Pressure transients detected with PVDF transducer in 2 mm distance to the ablated area. The distance between the distal fiber tip and the foot plate surface was 500 µm (noncontact). (**a**) Typical temporal intensity profile of the laser pulse. (**b**) Pressure signal during bone ablation with a laser fluence of 40 J/cm^2. (**c**) Pressure transients induced by a laser pulse (fluence 40 J/cm^2) applied through the fenestration directly into the artifical perylimph. The maximal value of the pressure peak at 235 µs rises up to 9 bar. (**d**) Pressure signal due to a laser pulse of 10 J/cm^2 directly applied to the artifical perylimph through the fenestration.

perforation of the stapes foot plate is demonstrated in Figure 5a. The pressure transients induced by the first laser spike is strongly pronounced compared to the ones of the following spikes. A comparison with the pressure signal induced in the noncontact mode (see Fig. 3, trace d) reveals that this strong first pressure transient appears only if the fiber is covered by water. A similar strong first pressure transient was found during bone ablation in the contact mode where the small gap between the fiber and the stapes foot plate is filled by water. It must, however, be mentioned that the pressure amplitudes induced by all the following laser spikes show independent whether the fiber is in contact or noncontact a comparable amplitude. The pressure signal

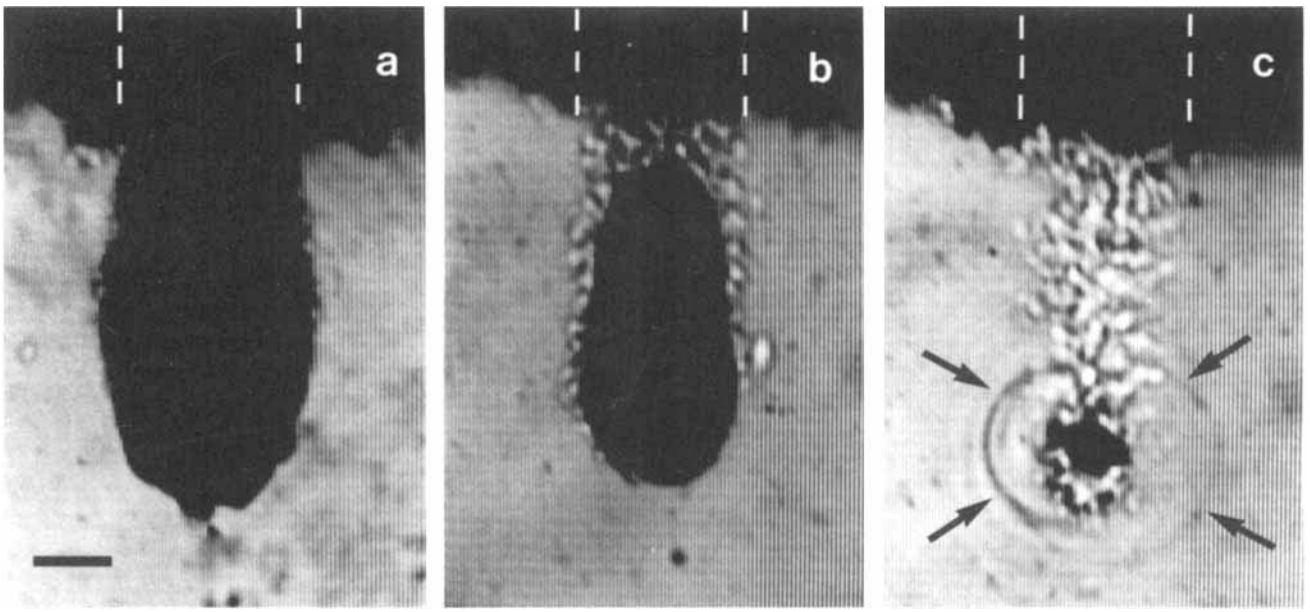

Fig. 4. Sequence of Schlieren optic pictures of the channel performed in the artifical perylimph of the inner ear model through the perforation of the foot plate taken at different times after the beginning of the laser pulse (fluence = 40 J/cm^2). The dashed white line represents the perforation (hole diameter 400 μm). Bar = 200 μm. (**a**) 145 μs: maximum size of the vapor channel. (**b**) 200 μs: the channel constrict under the bone surface and it separates a vapor bubble. The dark streaks around the vapor bubble indicate remaining turbulent warm water. (**c**) 240 μs: a shock wave results due to the collapse of the channel. The shock front is marked by arrows.

measured at 100 μs and 180 μs again are due to the channel collapse, and the one at 200 μs originates from a collapse after rebound of the bubble. For low laser fluence of 10 J/cm^2, the vapor channel collapses during the laser pulse, although there is still laser radiation. It is remarkable that the maximal pressure amplitudes of both the pressure peak induced by the explosive vaporisation at the beginning of the laser pulse and the pressure peak induced by the collapse is limited to ~500 mbar if the laser fluence is kept below 10 J/cm^2. Figure 5b shows the beginning of both signals at a faster timescale. Each laser spike leads to a single pressure transient. The time delay between the individual laser spikes and the pressure transients is the time, the pressure waves needs to pass the distance between the place of generation and the PVDF detector.

Figure 6 shows the relation between the maximal pressure amplitude measured during the bone ablation process in the artificial perilymph at a distance of 2 mm under the bone surface and the laser fluence at the fiber. The straight line with the larger slope is the absolute pressure amplitude of the strong first pressure transient that appears if the fiber is in contact. The straight line with the smaller slope represents the amplitude of the pressure transients resulting from all the other laser spikes. These pressure amplitudes show the same value for the contact as well as for the noncontact mode. Each

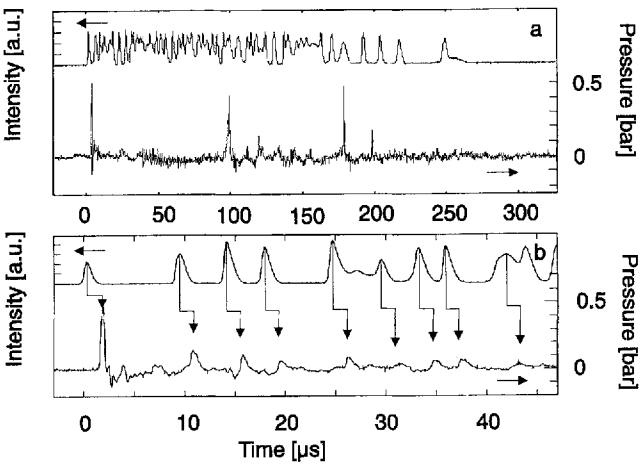

Fig. 5. (**a**) Temporal intensity profile and induced temporal pressure signal of a laser pulse (fluence = 10 J/cm^2) applied in contact directly to the artifical perylimph of the inner ear model. (**b**) Zoomed area of the first 50 μs. The arrows indicate the temporal correlation between the individual spikes of the laser pulse and the corresponding pressure transients.

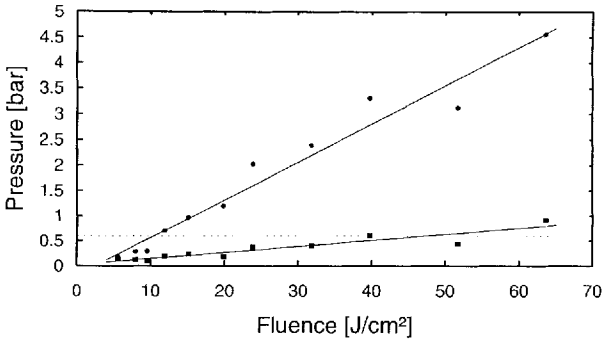

Fig. 6. Maximum pressure amplitudes as a function of the laser fluence measured during the bone ablation in contact mode (●): induced by the first laser spike, (■): induced by the following laser spikes. Each experimental point is an average of five measurements.

data point represents the average of five measurements.

Morphology

The scanning electron microscopic evaluation showed a round perforation with sharp edges and no evidence of charring or signs of melted bone material (Fig. 7a,b). The magnification of the ablation site drilled with five pulses at a fluence of 12 J/cm^2 shows the natural structure of the hard-bone components. The crystalline clusters are recognised.

Histology of the laser-treated and perforated human stapes revealed a thin zone of thermally damaged bone tissue measuring always <10 μm (Fig. 8a,b).

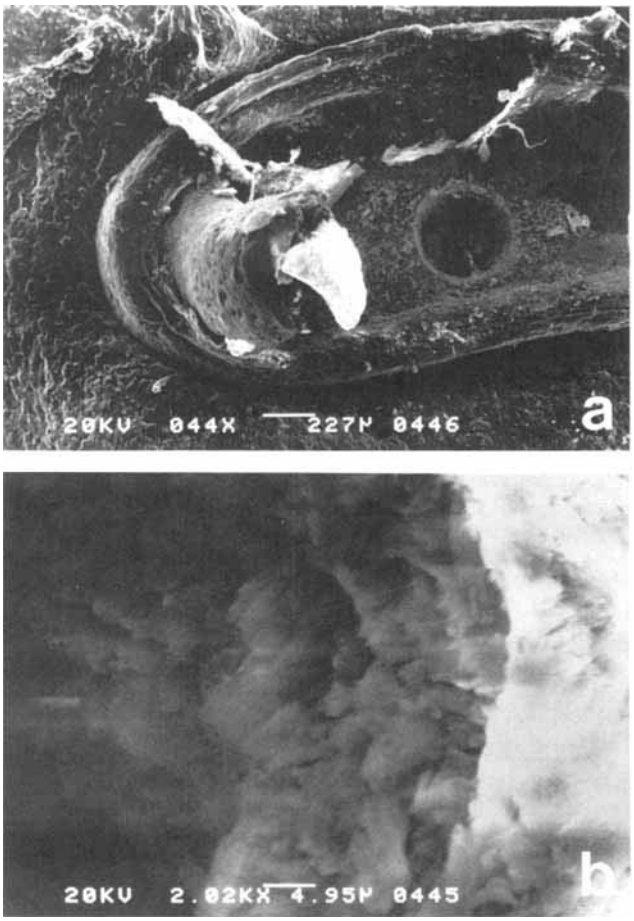

Fig. 7. (**a**) Scanning electron microscopy revealed a very precise circle hole in a human stapes foot plate. The hole was drilled with 5 pulses of 12 J/cm^2 measured at the fiber tip (core diameter of 400 μm). (**b**) No melted bone material is visible at the crater edges of the perforation.

DISCUSSION

Laser-assisted stapedotomy has the following potential risks associated with hole drilling in the stapes foot plate using pulsed laser radiation: (1) a temperature rise in the vestibule due to heat diffusion, (2) damage of organs lying behind the foot plate in the direction of the laser beam by direct irradiation, and (3) the destruction of the sensory hair cells by high intensity acoustic waves coupled directly into the vestibule due to the explosive ablation process. The results of this study show that all these risks can be avoided using an erbium laser with appropriate laser parameters, and a sharp round fenestration of the desired diameter can be achieved with a few laser pulses.

Temperature

Scanning microscopy of the crater edges shows no evidence of melted bone material, as is found, e.g., after Argon, CO_2, or Holmium laser interaction [17,20,21]. This means that the temperature during the ablation process was lower than the melting temperature of hydroxyaphatite, which is ~1,500°C. This corresponds well with direct temperature measurements on bone disks following erbium laser ablation [17], where we found a maximum temperature at the ablation site of ~350°C with comparable laser parameters. Additionally, the histological evaluation of treated foot plates revealed a thermally damaged zone of <10 μm around the edge of the perforation (see Fig. 8b). This confirms that the temperature rise at the ablation site is limited to a very local

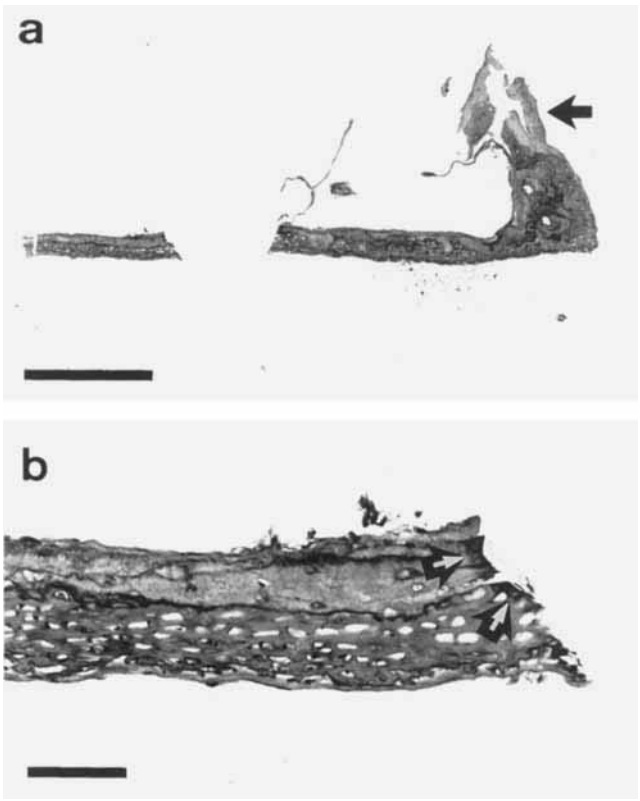

Fig. 8. Histology of a human stapes treated with 12 J/cm^2 using 5 laser pulses. (**a**) The two parts of the foot plate are seperated by a precise drilled hole. Parts of one of the crus are visible (→). Bar = 500 μm. (**b**) Higher magnification of the laser treated area reveals a small thermally damaged zone of 5 to 10 μm (marked by arrows). Bar = 100 μm.

volume. Temperature measurements performed in the inner ear model have shown that ablation following erbium laser treatment is not subject to appreciable heating in the artificial perilymph [20]. Therefore thermal damage of the inner ear due to erbium laser stapedotomy is very unlikely.

Direct Irradiation of Inner Ear Structures

Because of the extremely high absorption of the erbium laser radiation in water, the liquid of the vestibule represents an efficient "backstop" for 3 μm radiation. This prevents the direct irradiation of deeper lying structures of the inner ear. The flash photography pictures reveal that the backstop is realised by absorbing the laser pulse energy to create a vapor channel in the liquid (see Fig. 4a). For laser fluences higher than 80 J/cm^2, however, the depth of this water vapor channel becomes sufficient to penetrate the entire liquid layer of ~2 mm. Water vapor shows compared to liquid water at 3 μm an extremely low absorption. Therefore laser radiation can be transmitted through this water vapor channel, and injury to other inner ear structures due to direct irradiation becomes possible [19].

Pressure

The strongest pressure transient (up to 10 bar) induced during the erbium laser-assisted stapedotomy was found after applying an additional laser pulse into an already existing fenestration of the stapes foot plate. This laser pulse creates a vapor channel in the perilymph liquid. After the end of the laser pulse, the vapor channel constricts at the very top (the interface between the bone and the liquid), due to fast condensation of water vapor at the inner surface of the channel, which leads to a separated vapor bubble (see Fig. 4b). The collapse of this vapor bubble is able to create a strong shock wave, which is identified acoustically by a strong pressure transient (Fig. 3 trace c) and visualised by the Schlieren photography (Fig. 4c). After collapse the bubble rebuilds again, forming a rebound that subsequently collapses, leading to a further pressure transient.

For low laser fluences, the condensation of the water vapor can exceed the evaporation rate leading to a complete closure and subsequent collapse of the bubble during the laser pulse (pressure transient at 115 μs in Fig. 3, trace d, and at 100 μs in Fig. 5a). Depending on the laser fluence and pulse length used, the remaining laser pulse energy forms a new channel [19] whose collapse is again associated with a strong pressure transient as indicated by the pressure signal at 190 μs in Figure 3 (trace d) and at 180 μs in Figure 5a.

The comparison between the pressure signal measured after noncontact and contact application shows that in addition to the pressure transients caused by the channel collapse, a strong pressure transient appears at the very beginning of the laser pulse, although the first spike of the laser pulse is not pronounced (compare Figs. 3d and 5b). This first strong pressure transient always exists if the fiber end is covered by a liquid film, even when the foot plate is not yet drilled through. This reveals that the explosive evaporation of the water at the fiber tip is a result of the superheating of a very thin layer of liquid water just below the fiber tip due to the lack of nucleation points and the confined situation. A comparable temporal pressure signal is found if the distal end of the fiber is submerged [18].

The clear correlation between each individual spike of the laser pulse and the pressure tran-

sients shown in Figure 5b infers that each individual laser spike contributes to the ablation process. This is in excellent agreement with earlier measurements where we found the same correlation between laser spikes and the temporal development of the ejected material above tissue surfaces when measuring with a pump probe technique [13].

To estimate the strain on sensory hair cells due to all the pressure transients caused either by the explosive ablation process or the imploding channel collapse induced in the inner ear during erbium laser stapedotomy, we took the limit graph to avoid hearing defect published by Pfander as a basis [22]. These limits for the time-dependent maximal acoustic stress are valid for intact human ears and sound pressures created and measured outside the ear. The tympano ossicular system amplifies the acoustic wave by a factor of ~20 to adapt the impedance difference between air and perilymph [23]. Because the induced pressure transients during laser stapedotomy are coupled directly into the inner ear, the threshold to avoid a permanent hearing loss can be increased by 25 dB up to 190 dB corresponding to a pressure amplitude of 600 mbar for acoustic transients shorter than 200 μs. However, the frequency range transmitted through the middle ear by the ossicular chain is between 20 Hz and 20 kHz, whereas the laser-induced pressure transients are found to be in the ultrasonic range. Whether the hair cells or other delicate inner ear structures will be mechanically damaged by these high frequencies coupled directly into the inner ear for pressure amplitudes not higher than 600 mbar, or whether this threshold can be further increased is still open to question, which can be answered only by in vivo experiments.

Under the assumption that the limit graph to avoid permanent hearing loss is also valid for high frequencies, the amplitude of the laser-induced pressure transients should not exceed 600 mbar.

Applying a laser fluence up to 40 J/cm^2, the resulting pressure amplitudes induced by the explosive bone ablation process are lower than 600 mbar (see Fig. 6). Depending on the thickness of the stapes foot plate, the perforation can be performed with 2–4 laser pulses (see Fig. 2). However, after an additional pulse applied to the perilymph, the pressure transient caused by the collapse of the thereby created vapor channel is more than ten times higher than the transients caused by the bone ablation. The magnitude of the collapse pressure depends strongly on the volume and the geometry of the separated vapor bubble, both of which depend on the pulse energy. Decreasing the pulse energy decreases the collapse pressure as seen in Figure 3 (trace d) and Figure 5a, where the collapse pressures are limited to <600 mbar for a laser fluence of 10 J/cm^2. Additionally, Figures 5a and 6 show that with a laser fluence of 10 J/cm^2, this admissible pressure limit is not exceeded even if the perforation of the stapes foot plate is performed in contact, where a liquid film of blood or rinsing water covers the distal fiber tip. This means that the whole perforation procedure can be performed safely and reliably with 8–16 single laser pulses, whereby the thermally damaged zone around the fenestration is limited to <10 μm. Furthermore, an iatrogenic injury of the Saccule or Utricle either by direct irradiation or by heat diffusion can be excluded.

CONCLUSION

The results of our experiments show that the erbium YSGG laser is a very precise and universal instrument for middle ear surgery. Because of its extremely small penetration depth in water containing tissue, the deposited energy is located in a very small volume. Therefore, it is possible to drill small precise thin holes (<400 μm) in sclerotic bone with a high ablation efficiency (10 μm per pulse at 10 J/cm^2) and a small thermal damage zone (<10 μm). The high absorption of the erbium laser in the water containing perilymph fluid prevents an iatrogenic damage of other inner ear structures through direct irradiation. In summary, using a fluence of 10 J/cm^2, erbium laser-assisted perforation of the stapes foot plate seems to be promising and reliable because neither a significant thermal damage nor a dangerous acoustic stress to the inner ear takes place during the laser application independent of whether the distal fiber tip is in contact to the stapes foot plate or not. In vivo experiments are in progress to confirm our experimental findings and to quantify the influence of the high frequency pressure transients on the mechanical damage of inner ear structures.

ACKNOWLEDGMENTS

The authors express gratitude to James Morris and Duco Jansen for their valuable discussions and help with the manuscript. We thank also A. Friedrich, A. Stähli, H. Hutmacher, E. Krähen-

bühl, and S. Binggeli for technical assistance. This work was supported in part by the Swiss Commission of the Encouragement of Scientific Research.

REFERENCES

1. Thoma J, Mrowinski D, Kastenbauer ER. Experimental investigations on the suitability of the carbon dioxide laser for stapedotomy. Ann Otol Rhinol Laryngol 1986; 95: 126–131.
2. Kautzky M, Trodhan A, Susani M, Schenk P. Infrared laser stapedotomy. Eur Arch Otorhinolaryngol 1991; 248(8):449–451.
3. Perkins R, Curto FS Jr. Laser stapedotomy: A comparative study of prostheses and seals. Laryngoscope 1992; 102:1321–1327.
4. Gherini S, Horn KL, Causse JB, McArthur GR. Fiberoptic argon laser stapedotomy: Is it safe? Am J Otol 1993; 14 (3):283–289.
5. Molony TB. CO_2 laser stapedotomy. J La State Med Soc 1993; 145(9):405–408.
6. Grossenbacher R. Die Chirurgie mit Laserstrahlen in der Othorhynolaryngologie: Experimentelle und klinische Studie. Inaugural dissertation, University Zürich, 1982, 121–139.
7. Lesinski SG, Palmer A. Laser for otosclerosis: CO_2 vs. Argon and KT-532. Laryngoscope 1989; 99:1–8.
8. Coker NJ, Ator GA, Jenklins HA, Neblett CR. Carbon dioxide laser stapedotomy: A histology study. Am J Otholarygol 1986; 7:253–257.
9. Thoma J, Unger V, Kastenbauer E. Functional impact of argon-laser on the cochlea of the guinea-pig. Laryng Rhinol Otol 1982; 61:473–476.
10. Gantz BJ, Jenkins HA, Kishimoto S, Fisch U. Argon laser stapedotomy. Ann Otol 1982;91:25–26.
11. Nuss RC, Fabian RL, Sarker R, Puliafito CA. Infrared laser bone ablation. Lasers Surg Med 1988; 8:381–391.
12. Zweig AD, Frenz M, Romano V, Weber HP. A comparative study of laser tissue interaction at 2.94 μm and 10.6 μm. Appl Phys B 1990; 47:259–267.
13. Frenz M, Zweig AD, Romano V, Weber HP. Dynamics in laser cutting of soft media. SPIE 1990; 1202:22–33.
14. Wüthrich S, Lüthy W, Weber HP. Optical damage thresholds at 2.94 μm im fluoride glass fibers. Applied Optics 1992; 31(27):5833–5837.
15. Helfer D. Endoscopic beam delivery systems for Erbium laser radiation. Diplomawork, Institute of Applied Physics, University of Bern, 1993.
16. Schoeffmann H, Schmidt-Kloiber H, Reichel E. Time-resolved investigations of laser-induced shock waves in water by use of polyvinylidenefluoride hydrophones. J Appl Phys 1988; 63(1):46–51.
17. Romano V, Rodriguez R, Altermatt HJ, Frenz M, Weber HP. Bone microsurgery with IR-lasers: A comparative study of the thermal action at different wavelengths. SPIE 1993; 2077:87–97.
18. Frenz M, Pratisto H, Ith M, Asshauer T, Rink K, Delacrétaz G, Romano V, Salaté RP, Weber HP. Transient photoacoustic effects induced in liquids by pulsed erbium lasers. SPIE 1994; 2134.
19. Ith M, Frenz M, Pratisto H, Altermatt HJ, Weber HP. Dynamics of laser-induced channel formation in water and influence of pulse duration on the ablation of biotissue under water with pulsed erbium laser radiation. Appl Phys B 1995; 59:621–629.
20. Frenz M, Romano V, Pratisto H, Weber HP, Altermatt HJ, Felix D, Grossenbacher R. Stapedotomy: New results of the erbium laser. In: ORL "Aktuelle Probleme der Otolaryngologie." Bern: Hans Huber Verlag, 1994, pp 335–343.
21. Forrer M, Frenz M, Romano V, Altermatt HJ, Weber HP, Silenok A, Istomyno M, Konov VI. Bone-ablation mechanism using CO_2 laser of different pulse duration and wavelength. Appl Phys B 1993; 56:104–112.
22. Pfander F. "Das Knalltrauma." Berlin: Springer Verlag, 1975, pp 56–80.
23. v. Békésy G. "Experiments in Hearing." New York: McGraw-Hill, 1960, pp 95–126.